

FAK in the nucleus prevents VSMC proliferation by promoting p27 and p21 expression via Skp2 degradation

Kyuho Jeong ¹, James M. Murphy ¹, Eun-Young Erin Ahn ², and Ssang-Taek Steve Lim ^{1*}

¹Department of Biochemistry and Molecular Biology, College of Medicine, University of South Alabama, 5851 USA Drive North, Room 2366, Mobile, AL 36688, USA; and ²Department of Pathology, O'Neal Comprehensive Cancer Center, University of Alabama at Birmingham, Birmingham, AL 35294, USA

Received 15 June 2020; editorial decision 2 April 2021; accepted 8 April 2021; online publish-ahead-of-print 11 April 2021

Aims

Vascular smooth muscle cells (VSMCs) normally exhibit a very low proliferative rate. Vessel injury triggers VSMC proliferation, in part, through focal adhesion kinase (FAK) activation, which increases transcription of cyclin D1, a key activator for cell cycle-dependent kinases (CDKs). At the same time, we also observe that FAK regulates the expression of the CDK inhibitors (CDKIs) p27 and p21. However, the mechanism of how FAK controls CDKs in cell cycle progression is not fully understood.

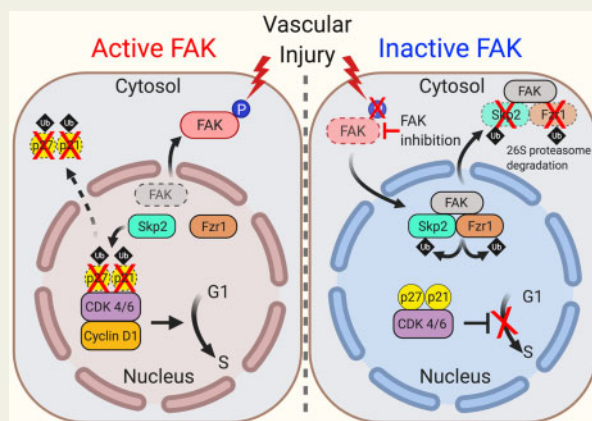
Methods and results

We found that pharmacological and genetic FAK inhibition increased p27 and p21 by reducing stability of S-phase kinase-associated protein 2 (Skp2), which targets the CDKs for degradation. FAK N-terminal domain interacts with Skp2 and an APC/C E3 ligase activator fizzy-related 1 (Fzr1) in the nucleus, which promote ubiquitination and degradation of both Skp2 and Fzr1. Notably, overexpression of cyclin D1 alone failed to promote proliferation of genetic FAK kinase-dead (KD) VSMCs, suggesting that the FAK-Skp2-CDKI signalling axis is distinct from the FAK-cyclin D1 pathway. However, overexpression of both cyclin D1 and Skp2 enabled proliferation of FAK-KD VSMCs, implicating that FAK ought to control both activating and inhibitory switches for CDKs. *In vivo*, wire injury activated FAK in the cytosol, which increased Skp2 and decreased p27 and p21 levels.

Conclusion

Both pharmacological FAK and genetic FAK inhibition reduced Skp2 expression in VSMCs upon injury, which significantly reduced intimal hyperplasia through elevated expression of p27 and p21. This study revealed that nuclear FAK-Skp2-CDKI signalling negatively regulates CDK activity in VSMC proliferation.

Graphical Abstract



Keywords FAK • Skp2 • Fzr1 • CDK • p27 • p21 • VSMC • Neointimal hyperplasia • vascular injury

1. Introduction

Vascular smooth muscle cells (VSMCs) are an essential component covering conduit arteries, which control vascular tone and blood pressure.¹ While VSMCs normally exhibit very low proliferative capacity, they become highly proliferative and migratory during diseased conditions including atherosclerosis and restenosis, resulting in a narrowed vessel lumen.^{2–4} Currently there are few treatments for narrowed vessels, most of which are limited to large conduit vessels. Since small vessels can also become narrowed and occluded in peripheral arterial disease, there is a need for developing new systemic treatment options.^{5–7}

VSMC proliferation is tightly controlled through transcription, translation, post-translational modification, and degradation of cell cycle regulators.^{8,9} While VSMCs in mature arteries normally stay at early G1 phase of the cell cycle,¹⁰ pathological stimuli induce G1-to-S phase transition and promote VSMC proliferation.¹¹ The G1-to-S phase transition is induced by the formation of cyclin D-cyclin-dependent kinase (CDK) 4/6 and cyclin E-CDK 2 complexes.¹² Binding of cyclins to CDKs promotes CDK activation resulting in phosphorylation of pRb and activation of E2F1, a key transcription factor in promoting G1-to-S transition.¹³ However, CDK inhibitors (CDKIs)—Ink4 families for CDK 4/6 and Cip/Kip families for CDK 4/6 and 2—can inactivate cyclin-bound CDKs, which adds to the complexity of cell cycle regulation.^{14,15} As such, both activation of cyclin-CDK complexes and repression of CDKIs are required to properly operate G1-to-S cell cycle progression by activating pRb protein.¹⁶ The CDKIs p27Kip1 (p27), p21Cip (p21), and p57Kip1 (p57) inhibiting CDK 2, 4, and 6 have been extensively studied in VSMCs.^{17–20} These Cip/Kip family CDKIs are regulated post-transcriptionally through ubiquitin ligase complexes such as the S-phase kinase-associated protein-1 (Skp1)-Cul1-F-box (SCF) complexes. Skp2 is the substrate-recognizing component of SCF^{Skp2} and is implicated in the polyubiquitination and proteasomal degradation of p27, p21, and p57.^{21–23}

Focal adhesion kinase (FAK) is a protein tyrosine kinase which transmits extracellular signals through integrin or growth factor receptors.^{24,25} Upon activation, FAK is autophosphorylated at tyrosine 397 (pY397), and pY397 FAK is used as an indicator of FAK activity.²⁶

Elevated FAK activation by increased extracellular matrix or growth factor stimulation associated with vessel injury has been implicated in VSMC proliferation.^{27–30} A recent report further demonstrated that FAK catalytic activity and subcellular localization regulate VSMC proliferation through GATA4-mediated transcription of cyclin D1.³¹ In healthy femoral arteries, FAK exhibited low activity and mainly localized in the nucleus of VSMCs. On the contrary, FAK was more active and present in the cytoplasm of VSMCs of injured arteries.³¹ As overexpression of cyclin D1 failed to rescue proliferation in VSMCs when FAK catalytic activity is inhibited,³¹ the notion that repressing CDKIs is also required to promote G1-to-S cell cycle progression^{17,32,33} prompted us to investigate an uncharacterized switch in CDK regulation by the Cip/Kip CDK family via FAK signalling.

In this study, we found FAK activity promotes VSMC proliferation through decreased expression of the CDKIs p27 and p21, independently of enhanced cyclin D1 transcription following FAK activation. Mechanistically, in quiescent VSMCs, inactive nuclear FAK forms a complex with Skp2 and fizzy-related 1 (Fzr1)—an activator for APC/C E3 ligase complex (also known as CDH1), leading to proteasomal degradation of both Skp2 and Fzr1. This increases the stability of p27 and p21 and reduces the proliferative capacity of VSMCs. On the contrary, in proliferating VSMCs, increased FAK activity and cytoplasmic localization result in elevated Skp2 expression which facilitates p27 and p21 degradation. This study uncovers that FAK activation is critical in VSMCs proliferation by activating CDKs through reduced CDKI p27 and p21 stability.

2. Methods

2.1 Reagents

Small-molecule FAK inhibitor VS-4718 (MedKoo), MG132 (S2619; Selleckchem), Leptomycin B (LC Laboratories), BrdU (#423401; Biologend), and recombinant human PDGF-BB (R&D Systems) were purchased. Antibodies were obtained from the following vendors: FAK (#05-537), PCNA (#PLA0080), and GAPDH (#MAB374) antibodies from MilliporeSigma; β -actin (#SC47778), p27 (#SC1641),

p21 (#SC6246), Fzr1 (#SC56312), GFP (#SC9996), and GST (#SC138) antibodies from Santa Cruz Biotech; pY397 FAK (#44-624 G), cyclin D1 (#MA5-16356), and Skp2 (#51-1900) antibodies from Thermo Fisher; α -SMA (#ab5694) and BrdU (#ab6326) antibodies from Abcam; PARP (#611038) antibody from BD Biosciences; pS807/811 pRb (#8564) antibody from Cell Signaling Technology; Ki-67 antibody (#RB-1510-P0) from Neomarkers; and Myh11 antibody (#BT-562) from Alfa Aesar.

2.2 Plasmid constructs

GFP-tagged FAK WT, FERM, kinase, and C-terminal domain plasmid were used as previously described.^{34,35} FAK FERM F1 (33-132), FERM F2 (128-253), and FERM F3 (253-353) lobes were amplified by PCR and cloned into the pEBG mammalian GST fusion expression vector as described.³⁵ Myc-tagged Skp2 (#19947) and HA-tagged Fzr1 (#11596) plasmid constructs were from Addgene. Two different shRNAs targeting mouse Skp2 were cloned into pSicoR-mCherry (Addgene #21907) using XhoI and HpaI restriction site. shRNA sequences for Skp2-1 and -2 are listed in *Online Table 1*.

2.3 Mice

All animal experimental procedures were approved by the Institutional Animal Care and Use Committee at the University of South Alabama and adhere to the National Institutes of Health Guide for the Care and Use of Laboratory Animals. As the Myh11-Cre-ER^{T2} transgene is expressed on the Y chromosome, only male mice were used for animal experiments. FAK wild-type (WT)/kinase-dead (KD) (FAK^{WT/KD}), FAK flox/flox (FAK^{FL/FL}), and VSMC-specific Cre mice (Myh11-Cre-ER^{T2}) were used in this study as described previously (*Supplementary material online, Figure S1*).³¹ Cre recombinase was activated by treating male mice (6 weeks old) with tamoxifen (75 mg/kg, intraperitoneal, every other day) for 2 weeks, generating FAK^{-WT}, Myh11-Cre-ER^{T2} (FAK-WT) and FAK^{-KD}, Myh11-Cre-ER^{T2} (FAK-KD) mice. For euthanasia, mice were anesthetized via intraperitoneal injection of ketamine/xylazine (100 mg/kg and 8 mg/kg, respectively) followed by terminal cardiac bleed.

2.4 Femoral artery wire injury model

Femoral artery injury was performed by wire insertion in male mice (8 weeks old) as described previously.³¹ Briefly, mice were anesthetized by a single intraperitoneal injection with a mixture of ketamine/xylazine (100 mg/kg and 8 mg/kg, respectively). Then the left femoral artery was exposed by blunt dissection, and a branch of the femoral artery was partially transected to allow the introduction of a straight wire (diameter, 0.38 mm). The wire was passed within the vessel three times and left for 1 min. The muscular branch was ligated, and the incision closed after removing wire. For FAK inhibitor experiments, mice were treated twice daily with vehicle (10 mM citrate, pH 6.0) or the FAK inhibitor VS-4718 (50 mg/kg) by oral gavage. For VSMC-specific FAK-WT and FAK-KD mice experiments, wire injury was performed after 2 weeks of tamoxifen injections. For Skp2 shRNA or Myc-Skp2 lentiviral infection of femoral artery, concentrated lentivirus (10⁷ transducing units) was mixed with nonionic surfactant (Pluronic F-127, Sigma-Aldrich) in PBS as described previously.³¹

2.5 Carotid artery ligation

The carotid artery ligation was performed in male mice (8–10 weeks old) as described previously.³⁶ Mice were anesthetized by a single intraperitoneal injection with a mixture of ketamine/xylazine (100 mg/kg and

8 mg/kg, respectively). The left carotid artery was exposed through fine forceps and ligated with 6–0 silk suture just below the carotid bifurcation. The mice were treated twice daily with vehicle (10 mM citrate, pH 6.0) or the FAK inhibitor VS-4718 (50 mg/kg) by oral gavage. After 2 weeks, arteries were excised and embedded in OCT compound for sectioning.

2.6 BrdU incorporation assay

Labelling of proliferating cells in wire injury mice was done by intraperitoneal injection of BrdU (50 mg/kg) 72, 24, and 2 h before euthanasia. For BrdU immunostaining, DNA in frozen sections of femoral artery was denatured with 2 N HCl for 30 min, neutralized with 0.1 M NaHCO₃ (pH 8.5) for 10 min before blocking, and then incubated with antibodies against BrdU and α -SMA.

2.7 Cell culture

Primary mouse thoracic aorta VSMCs were isolated from 6- to 8-week-old male C57BL/6, FAK^{FL/FL}, FAK^{FL/WT}, and FAK^{FL/KD} mice. Isolated FAK^{FL/WT} and FAK^{FL/KD} VSMCs were treated with Cre adenovirus (50 MOI) to generate FAK-WT and FAK-KD VSMCs. Isolated VSMCs were verified for expression of different SMC-specific markers such as α -SMA and Myh11, and only used up to passage 6 (*Supplementary material online, Figure S2*). VSMCs, HEK293T, and HEK293FT cells were grown in DMEM supplemented with 10% FBS at 37°C with 5% CO₂. Human coronary artery SMCs (hCASMCs) were purchased (#CC2583, Lonza) and grown in SMC growth basal medium (SmBM, Lonza) supplemented with 5% FBS and additional growth medium (SmGM-2 SingleQuots, Lonza) according to instructions from the supplier.

2.8 Lentivirus production and generation of stable cell lines

Lentivirus was produced as previously described.³¹ Briefly, HEK293FT cells were transfected with third-generation packaging system using PEI reagent (Polysciences). At 72 h after transfection, lentivirus-containing medium was centrifuged to remove cell debris and passed through a 0.45- μ m filter (Steriflip-HV PVDF, Millipore). The lentivirus was concentrated using Amicon Ultra-15 Centrifuge Filter Unit (100,000 Dalton cut-off, Millipore). For generation of stable cell lines, VSMCs were incubated with purified lentivirus (20 MOI). For Skp2 and cyclin D1 overexpression, VSMCs were treated with puromycin (2 μ g/ml) 48 h after transduction. FAK^{FL/FL} VSMCs were transduced with FLAG-tagged FAK-WT (FLAG-FAK-WT) or nonnuclear localizing mutant (FLAG-FAK-NLM, R177A/R178A) and selected using puromycin. Endogenous FAK flox alleles were removed following treatment with Cre adenovirus (50 MOI). Stable expressing cells were used in experiments. For *in vivo* use, lentivirus was concentrated by ultracentrifugation at 25,000 rpm for 1.5 h (SW40-Ti rotor, Beckman Coulter), and lentivirus was resuspended in sterile PBS.

2.9 Cell proliferation

Mouse VSMCs (1 \times 10⁵ cells) were seeded on 0.1% gelatin-coated 6-well culture dishes. At 24 h intervals, cells were dissociated with 0.25% trypsin-EDTA (Sigma-Aldrich) and were mixed with trypan blue, and counted using the Countess II FL Automated Cell Counter (Life Technologies). Proliferating VSMCs was also evaluated through staining of a proliferation marker Ki-67. Three independent experiments were performed.

2.10 Western blotting

Cells and arteries were lysed with RIPA buffer (pH 7.4) that contains 4-(2-hydroxyethyl)-1-piperazineethanesulfonic acid (HEPES; 50 mM), NaCl (150 mM), Triton X-100 (1%), sodium deoxycholate (1%), sodium dodecyl sulphate (SDS; 0.1%), glycerol (10%), and protease inhibitors (Protease Inhibitor Cocktail, Roche). Lysates were cleared by centrifugation, and equal amounts of proteins were separated by SDS-PAGE and immunoblotted with indicated antibodies. All immunoblots were repeated at least three times. Blots were quantitated using ImageJ densitometry plugin and normalized using loading control.

2.11 Immunoprecipitation

VSMCs were treated with/without VS-4718 (2.5 μ M) together with MG132 (20 μ M) for 6 h and lysed with immunoprecipitation buffer that includes Triton X-100 (1%), HEPES (50 mM), NaCl (150 mM), glycerol (10%), ethylene glycol tetraacetic acid (1 mM), sodium pyrophosphate (10 mM), sodium fluoride (100 mM), sodium orthovanadate (1 mM), and complete protease inhibitor cocktail (Roche). For HEK293T cells, cells were transfected with GFP-tagged FAK constructs,³⁵ Myc-Skp2, and HA-Fzr1 for 48 h and lysed with the immunoprecipitation buffer. Lysates were cleared by centrifugation, and equal amounts of proteins were subjected to immunoprecipitation with indicated antibodies. The lysates were rotated overnight at 4°C, then protein G or A agarose beads were added, and the mixture was rotated for 2 h at 4°C. The immunocomplexes were washed three times with immunoprecipitation buffer and suspended with 2X SDS-loading buffer. Samples were separated by SDS-PAGE and immunoblotted with indicated antibodies.

2.12 GST pulldown assay

pEBG-FERM F1, F2, and F3 subdomain constructs, Myc-Skp2, and HA-Fzr1 were transfected in 293T cells. GST-FERM subdomains were pulled down using glutathione beads to determine their interaction with Skp2 and Fzr1.

2.13 Nuclear fractionation

Nuclear fractionation was performed as described previously.^{31,35} Briefly, VSMCs were treated with/without VS-4718 (2.5 μ M) together with MG132 (20 μ M) for 6 h and lysed with Cyto Buffer (10 mM Tris pH 7.5, 0.05% NP-40, 3 mM MgCl₂, 100 mM NaCl, 1 mM EGTA, 1 mM orthovanadate, and 1x protease inhibitor cocktail (Roche)), transferred into tubes, incubated for 5 min at 4°C, spun at 800 \times g at 4°C (5 min), and cytosolic supernatants collected. Cell pellets were further washed with Cyto Buffer, purified nuclei resuspended in RIPA buffer, spun at 16,000 \times g for 15 min, and the supernatant collected as the nuclear fraction. Cytosolic and nuclear lysates were boiled in SDS loading buffer, separated by SDS-PAGE, and immunoblotted with GAPDH as cytosolic marker and PARP as nuclear marker.

2.14 RNA isolation and real-time quantitative PCR (RT-qPCR)

Total RNA was extracted with TRIzol reagent (Life Technologies) and converted to cDNA using random hexamers and reverse transcription (Superscript III, Life Technologies). RT-qPCR was performed (iTaQ Universal SYBR Green SMX and CFX connected optical module, Bio-Rad). The sequences of RT-qPCR primers are listed in *Online Table 1*. All RT-qPCR was repeated three times, and mean \pm SEM was used as an error bar.

2.15 Immunostaining

Frozen sections or coverslips-grown cells were fixed with 4% paraformaldehyde 10 min. Samples were permeabilized with 0.1% Triton X-100 for 10 min, washed with PBS, and incubated with blocking solution including 1% BSA and 1% goat serum for 1 h at RT. The sections or coverslips were incubated with primary antibodies for overnight at 4°C. Samples were washed with PBS and incubated with conjugated goat anti-rabbit, anti-mouse, or anti-rat secondary antibodies (1:1000) (Alexa Fluor 594 or 488, Thermo Fisher) for 1 h at RT. Species-specific IgG or secondary antibodies were used as negative control. Slides were mounted using VECTASHIELD Antifade mounting medium (Vector Laboratories), and images were acquired with a confocal microscope at 60-fold magnification (Nikon A1R, Nikon). Images were processed using Photoshop CS5.

2.16 Statistical analysis

Data sets underwent Shapiro–Wilk test for normality, and statistical significance between experimental groups was determined with Student t-test or two-way analysis of variance (two-way ANOVA) with Sidak multiple comparisons test (Prism software, v7.0d; GraphPad Software). Power analyses were performed to determine sample size for two-way ANOVA. Blinding procedures were not employed in this study due to the following reasons: high reproducibility, noticeable differences between specimen, and data acquisition by quantification.

3. Results

3.1 FAK inhibition prevents VSMC proliferation by increasing the CDKIs p27 and p21

We have demonstrated that FAK catalytic activity and cellular localization regulate the transcription of cyclin D1 to promote VSMC proliferation.³¹ However, we also observed that cyclin D1 overexpression was not sufficient to promote VSMC proliferation under FAK inhibition. Since cyclin D-CDK4/6 complexes are inhibited by binding to CDKIs p27 and p21,³⁷ we tested whether this inhibitory pathway is altered upon FAK inhibition. We found that pharmacological FAK inhibition (VS-4718, 2.5 μ M) increases p27 and p21 protein expression ([Supplementary material online, Figure S3A](#)) and reduces VSMC proliferation as determined by cell counting and staining for Ki-67 positive cells ([Supplementary material online, Figures S3B and S4A](#)). FAK inhibition was confirmed by performing anti-pY397 FAK blotting ([Supplementary material online, Figure S3A](#)). We also tested effect of FAK inhibition in VSMC proliferation under PDGF stimulation. While PDGF increased the number of Ki-67 positive VSMCs, FAK inhibitor (FAK-I) treatment blocked PDGF-induced VSMC proliferation ([Supplementary material online, Figure S4B](#)). As FAK-I did not lead to increased mRNA expression of p27 and p21 ([Supplementary material online, Figure S3C](#)), we further verified FAK-I-mediated increase of p27 and p21 protein using a transcriptional inhibitor actinomycin D (ActD). While FAK-I did not alter p27 and p21 mRNA ([Supplementary material online, Figure S5A](#)), FAK-I still increased p27 and p21 protein expression even in the presence of ActD ([Supplementary material online, Figure S5B](#)). To confirm the observation that FAK inhibition increased p27 and p21 protein stability, VSMCs were treated with a protein synthesis inhibitor cycloheximide (CHX). While CHX rapidly reduced protein expression of p27 and p21, co-treatment with FAK-I increased the stability of p27 and p21 ([Supplementary](#)

material online, Figure S5C). VSMCs treated with FAK-I also showed decreased phosphorylation of pRb (Supplementary material online, Figure S6), confirming that elevated p27 and p21 proteins inhibit CDK4/6 activity. To rule out potential off-target effects of FAK-I, we used genetic FAK kinase-dead (KD) VSMCs (Supplementary material online, Figure S1) to test changes in p27 and p21. FAK-KD VSMCs exhibited increased p27 and p21 protein levels and reduced proliferation compared to FAK wild-type (WT) VSMCs (Supplementary material online, Figures S3D, E, and S4C). p27 and p21 mRNA levels were similar between FAK-KD and FAK-WT VSMCs (Supplementary material online, Figure S3F), suggesting that both pharmacological and genetic FAK inhibition increases p27 and p21 protein expression through post-transcriptional regulation.

3.2 FAK regulates p27 and p21 expression via reducing Skp2 stability

It is known that FAK regulates the stability of several nuclear proteins through direct binding.^{35,38–40} However, we did not observe a direct interaction between FAK and p27 or p21 (Supplementary material online, Figure S7). Since FAK-I reduced p27 and p21 protein level, we next looked at FAK regulation of Skp2, the substrate recognition component of the SCF^{Skp2} E3 ligase complex which targets p27 and p21 for degradation.^{21,22} FAK-I significantly reduced Skp2 protein expression in VSMCs from day 1 (Figure 1A). However, FAK-I did not affect Skp2 mRNA levels, indicating FAK may regulate Skp2 protein stability (Figure 1B). This was further verified by co-treatment with FAK-I and CHX, which led to accelerated loss of Skp2 protein than CHX alone (Supplementary material online, Figure S5C). FAK-I treatment in human coronary artery SMCs (hCASMCs) also reduced Skp2 expression with concomitant increases in p27 and p21 (Figure 1C), indicating that FAK regulation of CDKs through Skp2 is conserved between mouse and human. Consistent with pharmacological FAK inhibition, FAK-KD VSMCs also demonstrated decreased Skp2 protein (Figure 1D), but not mRNA levels compared to FAK-WT (Figure 1E). To confirm the possibility whether FAK inhibition reduced Skp2 stability, VSMCs were treated with FAK-I with/without a proteasomal inhibitor, MG132. While FAK-I alone reduced Skp2 levels, co-treatment with FAK-I and MG132 failed to reduce Skp2 (Figure 1F). These results demonstrate that FAK inhibition promotes Skp2 ubiquitination and proteasomal degradation. Immunostaining of vehicle-treated VSMCs showed that FAK is mainly localized in adhesions and cytosol with high levels of active pY397 FAK (Figure 1G). This was associated with strong nuclear staining of Skp2 and low levels of p27 and p21 (Figure 1G). Upon FAK-I treatment, we observed increased FAK nuclear localization with reduced levels of active pY397 FAK (Figure 1G). FAK-I treated VSMCs showed reduced Skp2 expression but elevated expression of p27 and p21 (Figure 1G and Supplementary material online, Figure S8A). PCNA staining was used as a proliferation marker (Figure 1G), and FAK inhibition indeed reduced PCNA expression. In agreement with pharmacological FAK inhibition, FAK-KD VSMCs showed elevated expression and nuclear localization of p27 and p21 compared to FAK-WT VSMCs (Supplementary material online, Figure S8B). Our results demonstrate that nuclear FAK reduces Skp2 stability and increases p27 and p21 expression to block VSMC proliferation.

3.3 FAK interacts with Skp2 and its E3 ligase activator Fzr1 via FAK FERM domain

To address a potential mechanism of how Skp2 protein stability is regulated by nuclear FAK, we performed Skp2 immunoprecipitation (IP) to test the possible association between Skp2 and FAK. We observed that

Skp2 interacts with FAK (Figure 2A), and additionally with Fzr1, a substrate recognition and activator of APC/C ubiquitin E3 ligase complex, known to target Skp2⁴¹ only when co-treated with FAK-I and MG132, but not in control (Figure 2A). Cytosolic and nuclear fractionation further showed that increased nuclear FAK and reduced Skp2 levels were observed after 6 h FAK-I treatment (Figure 2B). We also unexpectedly observed decreased Fzr1 protein upon FAK-I treatment. However, cotreatment with FAK-I and MG132 prevented loss of Skp2 and Fzr1 protein in the nucleus (Figure 2B). GAPDH and PARP were used to verify cytosolic or nuclear fractions, respectively (Figure 2B). To determine which FAK domain(s) associates with Skp2 or Fzr1, we performed overexpression studies in 293T cells using GFP-tagged FAK full-length (WT), FERM, kinase, or C-terminal constructs along with Myc-Skp2 and HA-Fzr1 (Figure 2C). GFP-IP showed similar levels of GFP-FAK construct expression and that both full-length FAK and FAK FERM interact with Skp2 and Fzr1 (Figure 2C). It is known that FAK FERM domain forms a scaffold by recruiting a substrate and its E3 ligase to promote protein degradation.^{35,38} We further examined which sublobes of FAK FERM acts as a scaffold to recruit Skp2 or Fzr1 by overexpressing GST tagged FERM sublobes F1, F2, and F3 in addition to Myc-Skp2 and HA-Fzr1 (Figure 2D). GST pulldown demonstrated that while Skp2 binds the FAK FERM F1 lobe, Fzr1 was able to interact with all three lobes with the strongest affinity for FERM F3 (Figure 2D). FAK-I treatment also decreased Fzr1 protein levels along with increased Skp2 degradation (Figure 2B and E). Neither pharmacological nor genetic FAK inhibition showed decreased Fzr1 mRNA levels (Figure 2F). These results indicate that the FAK FERM domain can serve as a scaffold for Skp2/Fzr1 ubiquitination and proteasomal degradation.

3.4 Both nuclear import and cytoplasmic export of FAK are critical for Skp2 and Fzr1 proteasomal degradation in the cytoplasm

As FAK is constantly shuttling between the cytoplasm and nucleus, it is possible that Skp2 and Fzr1 degradation occurs in either the nucleus or cytoplasm. To determine whether Skp2 and Fzr1 degradation occurred in the cytoplasm or in the nucleus, VSMCs were treated with FAK-I and a nuclear export inhibitor, Leptomycin B. Immunofluorescence showed that Skp2 and Fzr1 exhibited strong nuclear localization in vehicle-treated VSMCs (Supplementary material online, Figure S9A). However, FAK inhibition alone decreased Skp2 and Fzr1 expression and showed some cytoplasmic localization (Supplementary material online, Figure S9A). In contrast, cotreatment with FAK-I and Leptomycin B strongly increased staining of Skp2 and Fzr1 in the nucleus (Supplementary material online, Figure S9A), which suggests that Skp2 and Fzr1 degradation may occur in the cytoplasm. To verify whether FAK nuclear localization is required for Skp2 and Fzr1 degradation, we compared Skp2 or Fzr1 expression upon FAK-I treatment in FLAG-tagged FAK-WT (FLAG-FAK-WT) and nonnuclear localizing mutant (FLAG-FAK-NLM, R177A/R178A) expressed in FAK^{-/-} VSMCs.³¹ FAK-NLM failed to decrease expression of either Skp2 or Fzr1 following FAK-I treatment (Supplementary material online, Figure S9B). Immunostaining demonstrated that FAK-NLM fails to enter the nucleus under FAK-I conditions, and there was no change in Skp2 and Fzr1 expression (Figure 2G). These data suggest that FAK nuclear localization is critical for priming degradation of Skp2 and Fzr1, and that their degradation may occur in the cytoplasm.

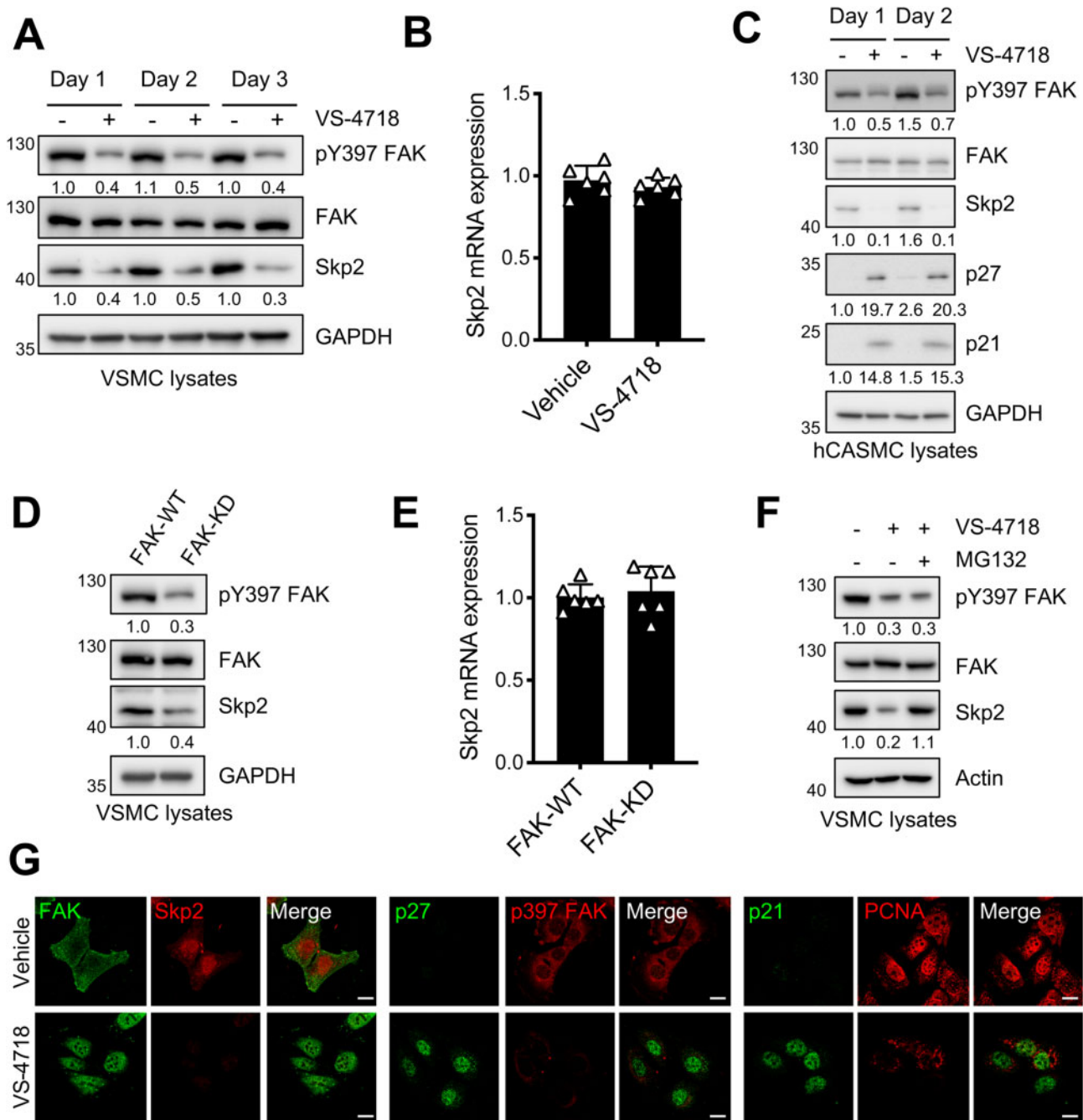


Figure 1 FAK inhibition reduces Skp2 expression by promoting nuclear localization of FAK. FAK inhibitor (VS-4718) was used at 2.5 μ M for the indicated times. (A, C, D, and F) Representative blots ($n = 3$). (A) Skp2 levels reduced upon pharmacological FAK inhibition monitored by immunoblotting with mouse VSMC lysates. Skp2 blots were quantified relative to GAPDH. pY397 FAK blots were quantified relative to total FAK. (B) Mouse VSMCs were treated with FAK inhibitor for 2 days, and Skp2 mRNA levels were measured via RT-qPCR (\pm SEM, $n = 6$, Student *t*-test). (C) Human coronary artery SMCs (hCASMCs) were treated with FAK inhibitor. Skp2, p27, and p21 blots were quantified relative to GAPDH. pY397 FAK was quantified relative to total FAK. (D) Skp2 levels in FAK-WT and FAK-KD mouse VSMCs. Skp2 blots were quantified relative to GAPDH. pY397 FAK blots were quantified relative to total FAK. (E) Skp2 mRNA levels were measured in FAK-WT and FAK-KD mouse VSMCs via RT-qPCR (\pm SEM, $n = 6$, Student *t*-test). (F) Mouse VSMCs were treated with FAK inhibitor with or without proteasome inhibitor (MG132, 20 μ M) for 6 h. Skp2 blots were quantified relative to actin. pY397 FAK was quantified relative to total FAK. (G) Mouse VSMCs were treated with or without FAK inhibitor for 24 h. FAK, Skp2, pY397 FAK, p27, and p21 immunostainings are shown. PCNA was used as a proliferation marker. Representative images ($n = 4$). Scale bar: 20 μ m.

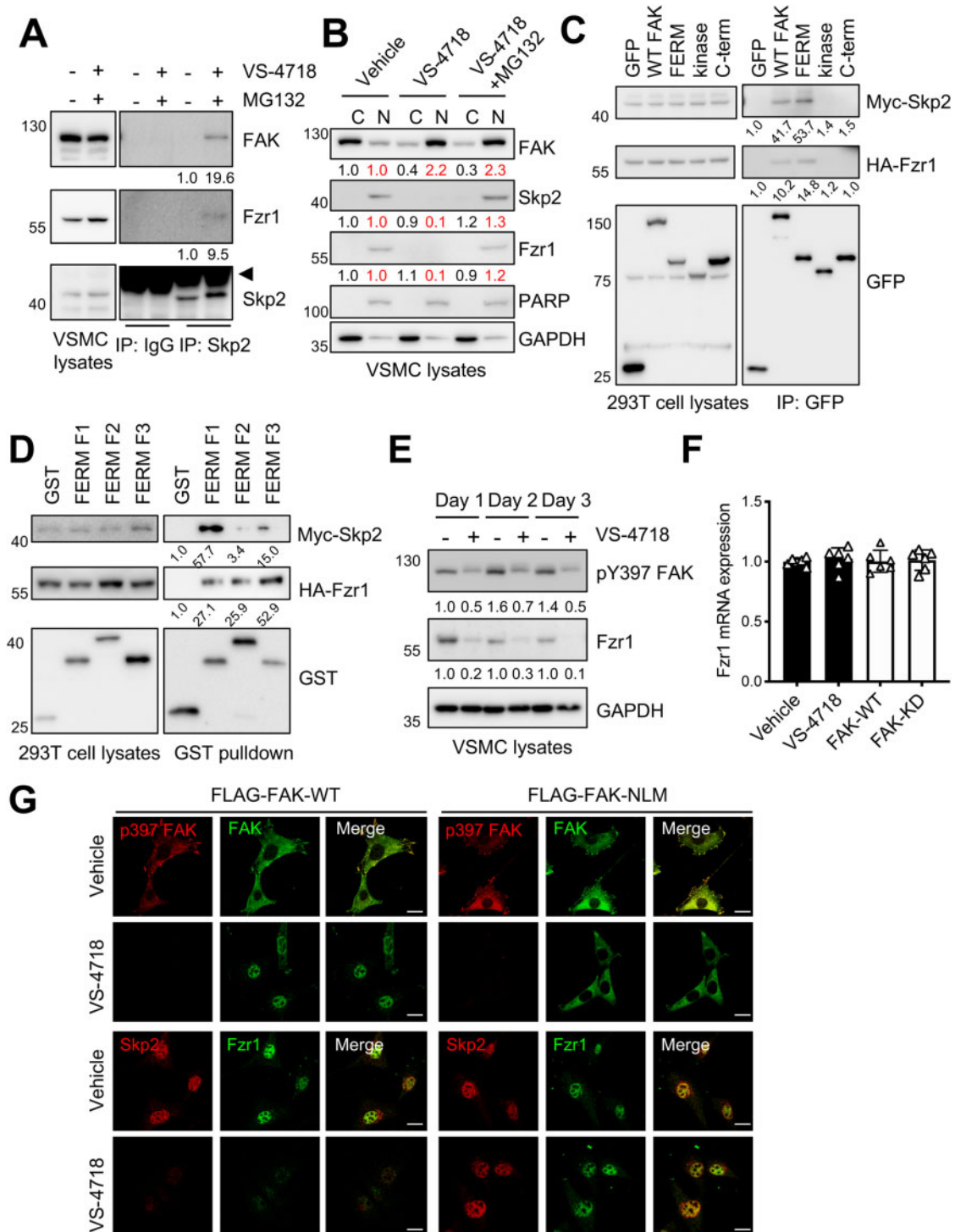


Figure 2 FAK interacts with Skp2 and the APC/C E3 ligase activator Fzr1 through FAK FERM domain. FAK inhibitor (VS-4718) was used at 2.5 μ M for the indicated times. (A–E) Representative blots ($n = 3$). (A) FAK interacts with Skp2 and Fzr1 by immunoprecipitation (IP) with VSMC lysates. Mouse VSMCs were treated with FAK inhibitor together with proteasome inhibitor (MG132, 20 μ M) for 6 h. FAK and Fzr1 blots within Skp2-IP were quantified relative to untreated controls. The arrow head indicates the heavy chain of IgG. (B) Immunoblots of mouse VSMC cytosolic (C) and nuclear (N) fractionated lysates for FAK, Fzr1, and Skp2. PARP and GAPDH as nuclear and cytosolic markers. Cytosolic or nuclear FAK, Skp2, and Fzr1 blots were quantified relative to GAPDH or PARP. (C) FAK FERM binds to both Skp2 and Fzr1 in 293T cells transfected with GFP-fused FAK and its subdomains. Skp2 and Fzr1 blots were quantified relative to GFP. (D) FAK FERM F1 lobe binds Skp2 and F3 lobe binds Fzr1 in 293T cells co-transfected with Myc-Skp2, HA-Fzr1, and FAK FERM F1, F2, and F3 lobes as GST fusion proteins. Skp2 and Fzr1 blots were quantified relative to GST. (E) Mouse VSMCs were treated with FAK inhibitor. pY397 FAK and Fzr1 blots were quantified relative to GAPDH. (F) Fzr1 mRNA levels were measured in mouse VSMCs treated with FAK inhibitor for 2 days or in genetic FAK inhibition via RT-qPCR (\pm SEM, $n = 6$, Student *t*-test). (G) Nuclear localization of FAK plays a key role in Fzr1 and Skp2 degradation. FAK^{-/-} mouse VSMCs stably expressing either FLAG-FAK-WT or -NLM were treated with VS-4718 for 12 h. Representative immunostaining with indicated antibodies ($n = 3$). Scale bar: 20 μ m.

3.5 Vascular injury-induced Skp2 expression and neointimal hyperplasia are blocked by pharmacological FAK catalytic inhibition

Because neointimal hyperplasia formation may vary significantly depending on the nature of vascular injury, we examined and compared the effects of FAK activity on Skp2-p27/p21 expression in neointimal hyperplasia and arterial remodelling using two different injury models. First, we used the femoral artery wire injury model. Since Skp2 was shown to reach its maximal level after 10 days and gradually returned to basal level after 28 days post carotid arterial balloon injury in rats,⁴² we collected femoral arteries 14 days post injury. Neointimal hyperplasia was determined using H&E staining (Figure 3A). While wire injury induced neointimal hyperplasia and significantly increased intima/media (I/M) ratio three-fold over sham in vehicle treated mice, mice treated with FAK inhibitor reduced neointimal hyperplasia and an I/M ratio similar to sham controls (Figure 3A). Immunoblotting of 14 day injured femoral artery lysates showed that wire injury increased levels of active pY397 FAK and Skp2, but reduced levels of p27 and p21 when compared with sham control (Figure 3B). However, VS-4718 treatment in injured arteries showed elevated levels of p27 and p21 when compared to injured vehicle (Figure 3B). Treatment with VS-4718 also reduced active pY397 FAK and Skp2 following wire injury (Figure 3B). In vehicle-treated sham mice, immunostaining of femoral arteries showed that FAK was localized to the nucleus and had no activity (pY397 FAK) and exhibited less Skp2 and Fzr1 expression (Figure 3C and Supplementary material online, Figure S10). We also observed abundant p27 and p21 in the nucleus (Figure 3C). In contrast, wire injury increased cytoplasmic FAK and active pY397 FAK, which was associated with elevated Skp2 and Fzr1, and loss of p27 and p21 (Figure 3C and Supplementary material online, Figure S10). VS-4718 treatment significantly inhibited pY397 FAK, Skp2, and Fzr1 expression in response to wire injury, and was able to restore p27 and p21 expression (Figure 3C and Supplementary material online, Figure S10).

To evaluate whether wire injury was triggering VSMC cell cycle progression from G1-to-S phase, we performed BrdU incorporation assay which monitors newly synthesized DNA.⁴³ In vehicle-treated mice, neointimal hyperplasia was gradually increased at 7 d and 14 d after wire injury, but was blocked by FAK-I treatment (Supplementary material online, Figure S11A). BrdU incorporation into α -SMA positive VSMCs was evaluated at 7 and 14 d post wire injury (Supplementary material online, Figure S11B). Throughout the time course, we observed increasing numbers of BrdU labelled VSMCs in the injured vehicle-treated femoral arteries compared to uninjured sham controls. Notably, FAK-I treatment was able to significantly reduce the number of BrdU-positive cells detected in the injured vessels. Together, these results suggest that FAK inhibition reduced neointima formation by increasing CDKIs and blocking VSMC entry into the cell cycle.

As wire injury may lead to thrombus formation and elevated endothelial activation, we next used the carotid artery ligation model to evaluate VSMC internal signalling pathways in remodelling. Carotid artery ligation led to robust neointimal hyperplasia formation in vehicle-treated mice, but was blocked in mice treated with FAK-I (Supplementary material online, Figure S12A). Artery ligation also led to increased Skp2 expression and loss of p27 in vehicle-treated mice (Supplementary material online, Figure S12B). In contrast, FAK-I trapped FAK in the nucleus and blocked ligation-induced increases in Skp2 and loss of p27 (Supplementary material online, Figure S12B).

3.6 VSMC-specific FAK-KD mice exhibit reduced hyperplasia with a low Skp2 and a high p27 and p21 expression after wire injury

In order to assess the role of FAK specific activity in VSMCs *in vivo*, we used a Cre/loxP strategy to create conditional VSMC-specific FAK-KD mice (Supplementary material online, Figure S1). Two weeks following femoral artery wire injury, VSMC-specific FAK-KD mice had a lower I/M ratio compared to FAK-WT mice (Figure 4A). Immunoblotting with artery lysates after wire injury clearly showed increased pY397 FAK and Skp2 levels along with decreased p27 and p21 expression in FAK-WT mice following wire injury (Figure 4B). However, VSMC-specific FAK-KD mice showed reduced levels in pY397 FAK and Skp2 upon wire injury, and restored levels of p27 and p21 compared to FAK-WT mice (Figure 4B). We further investigated changes in FAK activity, nuclear FAK, and expression of Skp2, Fzr1, p27 or p21 by performing immunostaining of femoral arteries. Wire injury increased expression of Skp2 and Fzr1, and reduced p27 and p21 levels in FAK-WT mice but not FAK-KD mice (Figure 4C). While wire injury relocalized FAK from the nucleus to cytoplasm in FAK-WT, FAK-KD showed abundant nuclear FAK in sham control and injured arteries (Figure 4C). Taken together, these results indicate that loss of FAK activity and increased nuclear localization of FAK inhibits neointimal hyperplasia through reduced expression of Skp2, resulting in elevated levels of p27 and p21.

3.7 Skp2 directly regulates CDKI expression and functions independently of cyclin D1 in the cell cycle progression

To verify the effect of Skp2 on p27 and p21 stability in VSMCs, we performed gain and loss of the function studies using lentiviral-mediated Skp2 overexpression or shSkp2 knockdown, respectively. Skp2 overexpression reduced p27 and p21 levels (Figure 5A) and slightly increased VSMC proliferation compared to control (Figure 5B). As expected, Skp2 overexpression had no effect on p27 and p21 mRNA levels (Figure 5C). On the contrary, Skp2 knockdown using shRNA increased p27 and p21 protein expression and significantly reduced VSMC proliferation (Figure 5D and F). Skp2 knockdown was verified by immunoblotting and RT-qPCR (Figure 5D and E). Loss of Skp2 did not change p27 and p21 mRNA levels (Figure 5E), confirming that Skp2-mediated p27 and p21 expression is regulated via ubiquitination/degradation pathway. Previously, we demonstrated that FAK catalytic inhibition blocked VSMCs proliferation through reduction of cyclin D1 transcription.³¹ However, we observed that overexpression of cyclin D1 did not promote VSMC proliferation in both FAK-I-treated and FAK-KD VSMCs (Supplementary material online, Figure S13), suggesting that cyclin D1 expression is necessary but not sufficient to fully activate CDK 4/6. As FAK inhibition also increased expression of CDKs p27 and p21 (Figure 2), it is possible that overexpression of both Skp2 and cyclin D1 could rescue VSMC proliferation during FAK inhibition. We generated dual overexpression of Skp2 and cyclin D1 in FAK-WT or FAK-KD VSMCs (Figure 5G and H). In striking contrast to overexpression of cyclin D1 alone, co-expression of Skp2 and cyclin D1 led to increased proliferation of both FAK-WT and FAK-KD VSMCs (Figure 5H). It is likely that reduction in p27 and p21 expression by overexpression of Skp2 in FAK-KD VSMCs enables cell cycle progression by releasing inhibitory regulation on CDK in the presence of cyclin D1 (Figure 5G). These data demonstrate that overexpression of

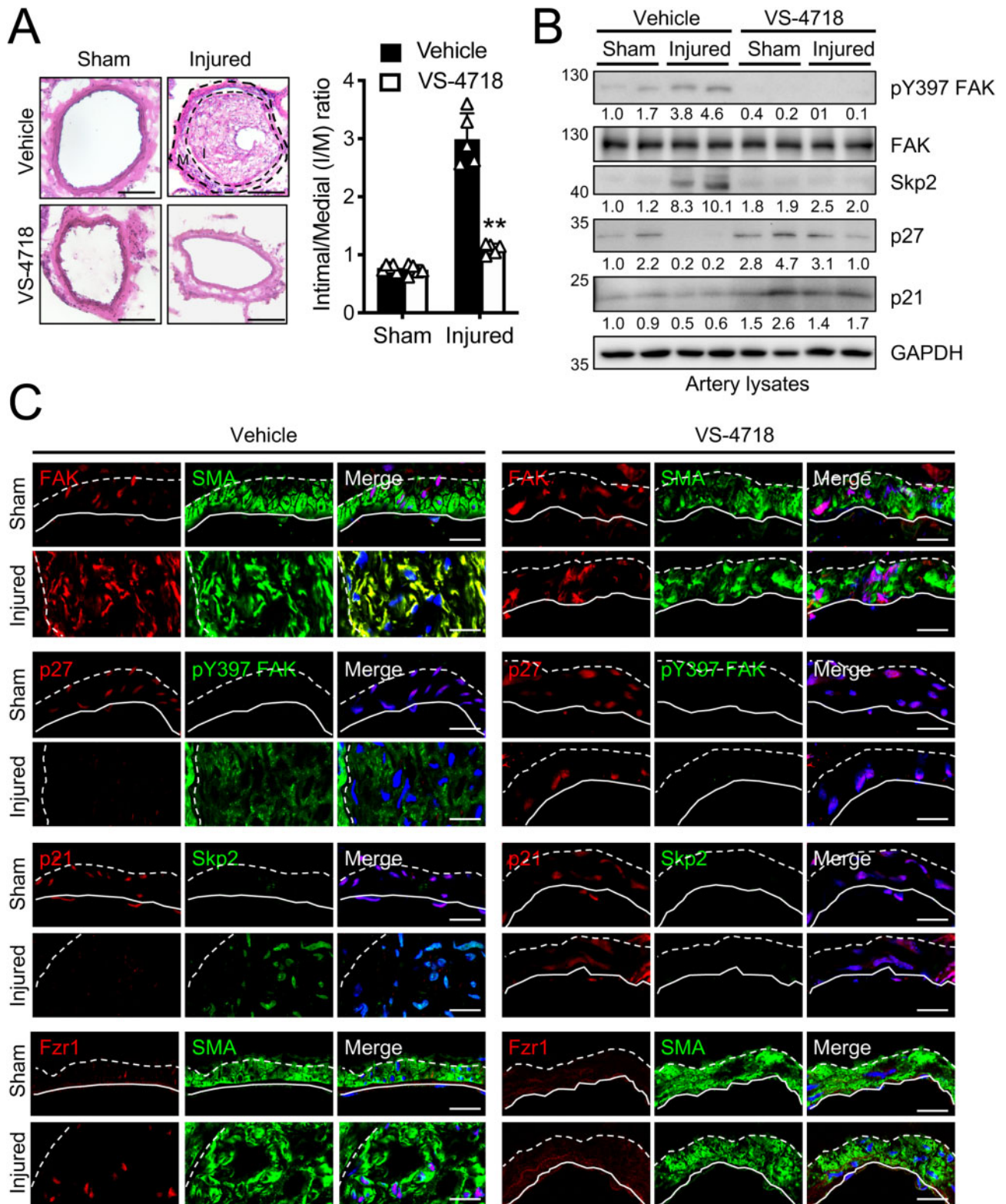


Figure 3 Skp2 is increased after wire injury and pharmacological FAK catalytic inhibition significantly reduces Skp2 and neointimal hyperplasia. Mice were treated with vehicle or VS-4718 (50 mg/kg) twice daily following wire injury. Representative H&E staining of femoral artery cross sections 14 days after wire injury for vehicle or VS-4718-treated (A, $n = 5$). Scale bar: 50 μ m. Intima/media (I/M) ratios were quantified (\pm SD, $n = 5$, $**P < 0.005$ vs. vehicle injury, two-way ANOVA followed by Sidak multiple comparisons test). (B) Representative immunoblots of femoral arteries 14 days postinjury for pY397 FAK, FAK, Skp2, p27, p21, and GAPDH as loading control. Skp2, p27, and p21 blots were quantified relative to GAPDH. pY397 FAK blots were quantified relative to total FAK. Representative blots ($n = 4$). (C) Representative immunofluorescence staining of femoral arteries 14 days postinjury for pY397 FAK, FAK, p27, p21, Skp2, Fzr1, and α -SMA. Red, green, and blue (DAPI) were merged ($n = 5$). Dotted line in image marks the external or internal elastic lamina. White line shows endothelial layer. Scale bar: 20 μ m.

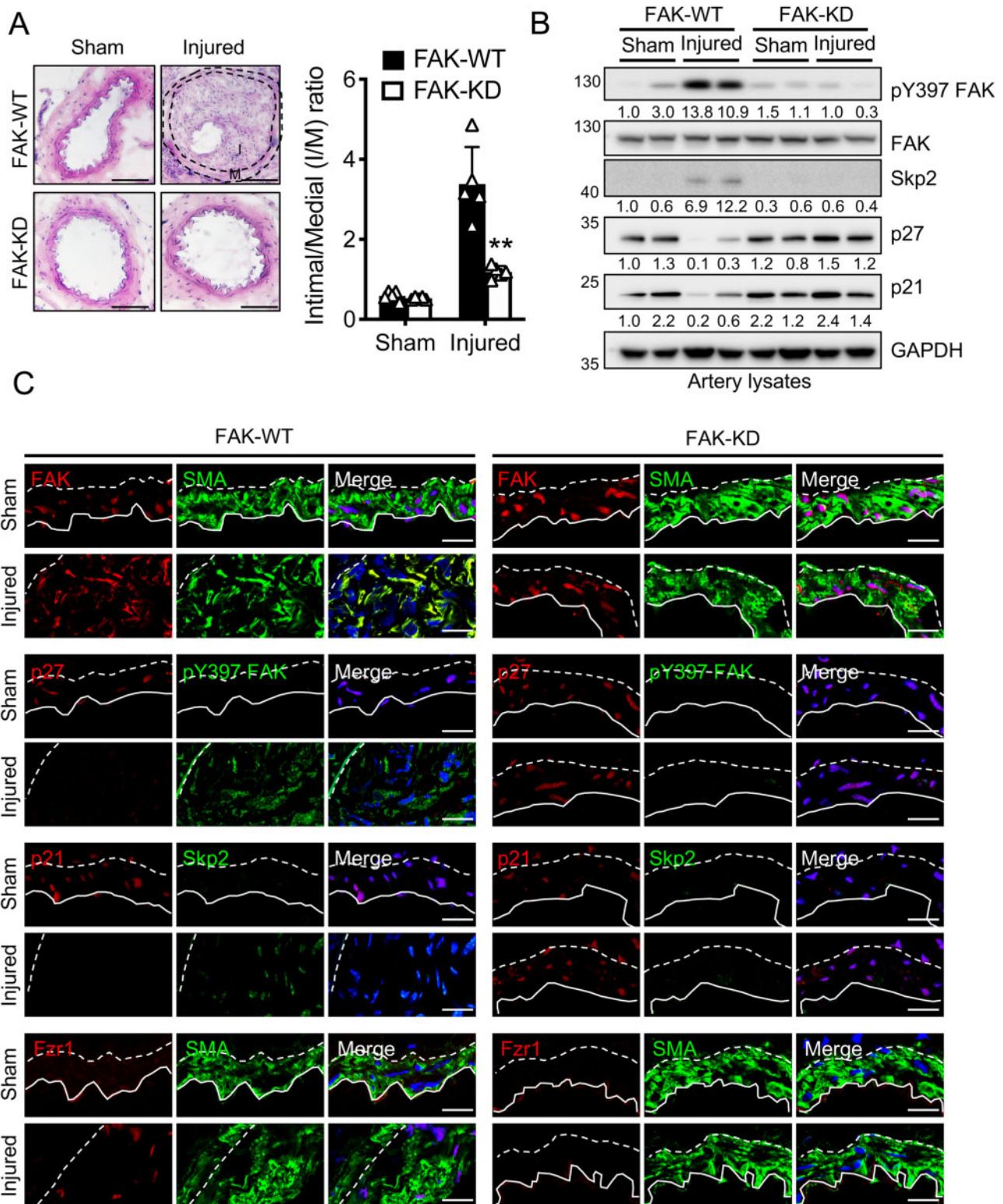


Figure 4 VSMC-specific FAK-KD mice development reduces hyperplasia and exhibits less Skp2 and more p27, p21 expression after wire injury. (A) Representative H&E staining of femoral artery cross sections 2 weeks after wire injury for genetic FAK-WT or FAK-KD mice ($n = 5$). Scale bar: 50 μm . Intima/media (I/M) ratios were quantified (\pm SD, $n = 5$, $**P < 0.005$ vs. FAK-WT injury, two-way ANOVA followed by Sidak multiple comparisons test). (B) Representative immunoblots of femoral arteries 14 days postinjury for pY397 FAK, FAK, Skp2, p27, p21 GAPDH as loading control. Skp2, p27, and p21 blots were quantified relative to GAPDH. pY397 FAK blots were quantified relative to total FAK. Representative blots ($n = 4$). (C) Representative immunofluorescence staining of FAK-WT and FAK-KD femoral arteries 2 weeks postinjury for pY397 FAK, FAK, p27, p21, Skp2, Fzr1, and α -SMA. Red, green, and blue (DAPI) were merged ($n = 4$). Dotted line in image marks the external or internal elastic lamina. White line shows endothelial layer. Scale bar: 20 μm .

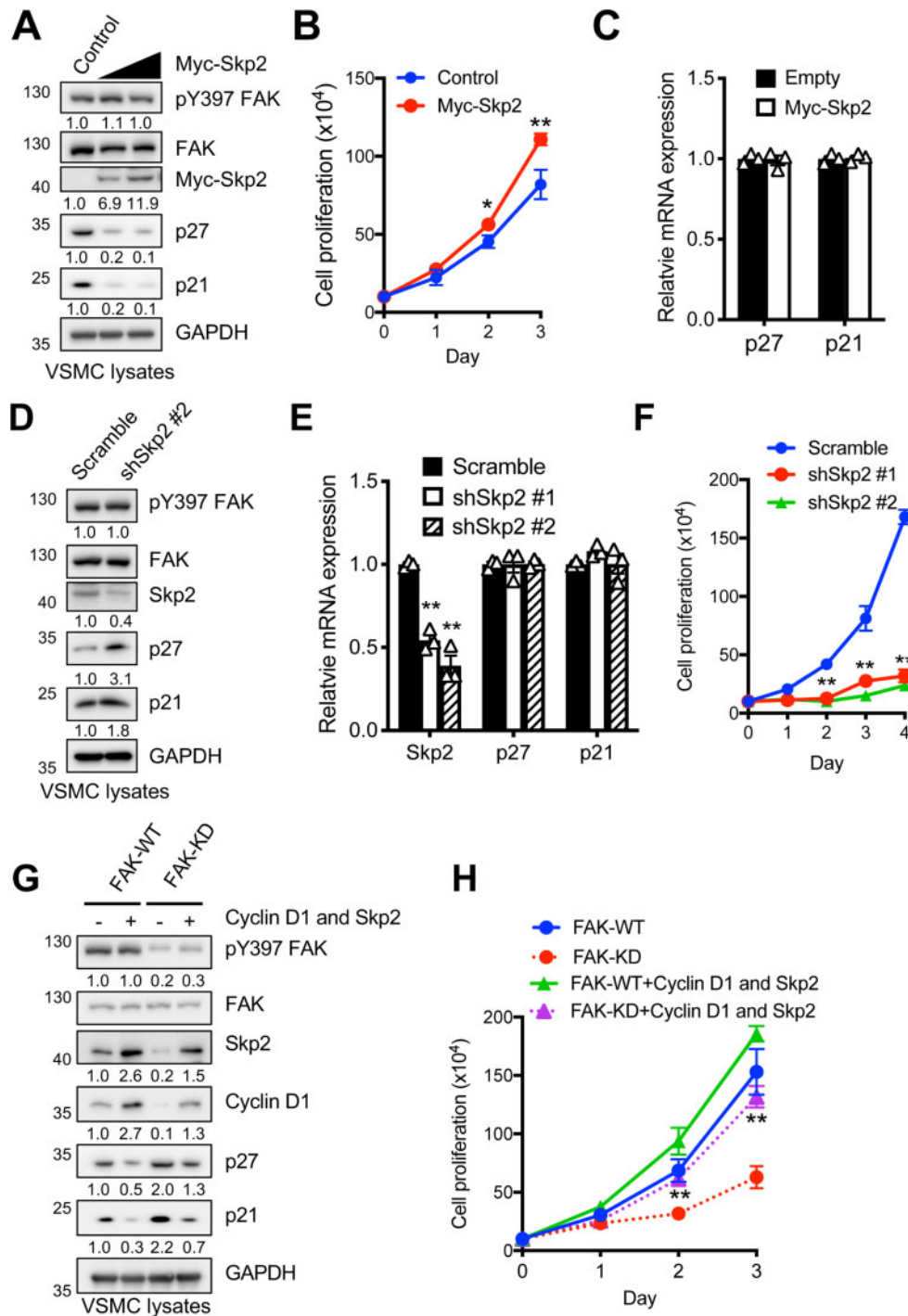


Figure 5 Skp2 directly regulates CDKI expression and functions independently of cyclin D1 in the cell cycle progression. (A) Mouse VSMCs were transfected to overexpress Skp2. Skp2, p27, and p21 blots were quantified relative to GAPDH. pY397 FAK blots were quantified relative to total FAK. Representative blots ($n = 3$). (B) Skp2 overexpression slightly increased mouse VSMC proliferation (\pm SD, $n = 3$, $*P < 0.01$, $**P < 0.005$ vs. control, two-way ANOVA followed by Sidak multiple comparisons test). (C) p27 or p21 mRNA levels were measured in mouse VSMCs overexpressing Skp2 via RT-qPCR (\pm SEM, $n = 3$, paired t -test). (D) shRNA-mediated knockdown of Skp2 increased p27 and p21 protein. Skp2, p27, and p21 blots were quantified relative to GAPDH. pY397 FAK blots were quantified relative to total FAK. Representative blots ($n = 3$). (E) Skp2, p27, and p21 mRNA levels were measured in Skp2 knockdown mouse VSMCs via RT-qPCR (\pm SEM, $n = 3$, $**P < 0.005$ vs. scramble, Student t -test). (F) Skp2 knockdown reduced mouse VSMC proliferation (\pm SD, $n = 3$, $**P < 0.005$ vs. scramble, two-way ANOVA followed by Sidak multiple comparisons test). (G) Cyclin D1 and Skp2 were overexpressed in FAK-WT and FAK-KD mouse VSMCs. Skp2, cyclin D1, p27, and p21 blots were quantified relative to GAPDH. pY397 FAK blots were quantified relative to total FAK. Representative blots ($n = 3$). (H) Skp2 overexpression rescues defect of mouse VSMCs proliferation in cyclin D1-overexpressing FAK-KD VSMCs (\pm SD, $n = 3$, $**P < 0.005$ vs. FAK-KD, two-way ANOVA followed by Sidak multiple comparisons test).

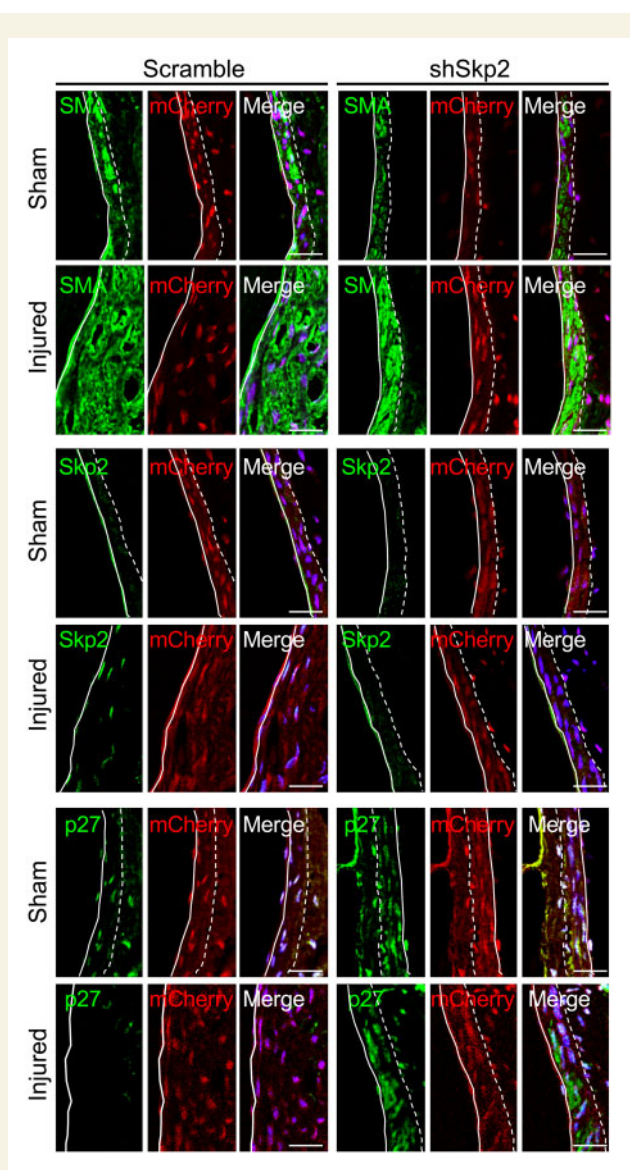


Figure 6 Knockdown of Skp2 reduces wire injury-induced neointimal hyperplasia. Femoral arteries were coated with either lentivirus encoding mCherry, scramble shRNA (shScr), or Skp2 shRNA (shSkp2) immediately following wire injury. After 2 week wire injury, immunostainings for α -SMA, Skp2, and p27 were shown. SMA (green), mCherry (red), and DAPI (blue) were merged ($n = 4$). mCherry was used to verify viral infection. Dotted line in image marks the external or internal elastic lamina. White line shows endothelial layer. Scale bar: 20 μ m.

both Skp2 and cyclin D1 can overcome FAK inhibition to promote VSMC proliferation by fully activating CDKs.

3.8 Skp2 knockdown reduces wire injury-induced neointimal hyperplasia

To verify the importance of Skp2 expression on VSMC proliferation *in vivo*, we knocked down Skp2 using shRNA (shSkp2). Lentivirus encoding mCherry and shSkp2 or scramble control (shScr) were mixed with Pluronic F-127 and pasted to the outside of femoral arteries immediately following surgery. Arteries were collected 2 weeks post-injury and analysed. Neointimal hyperplasia was significantly reduced in shSkp2 mice

compared to shScr (Supplementary material online, Figure S14A). Lentiviral delivery was verified through mCherry expression within femoral arteries (Figure 6 and Supplementary material online, Figure S14B). Skp2 knockdown blocked wire injury-induced upregulation of Skp2 but increased p27 expression (Figure 6 and Supplementary material online, Figure S14C, D). While shSkp2 reduced neointimal hyperplasia, wire injury still increased FAK cytoplasmic localization and activation (Supplementary material online, Figure S15), further supporting the notion that increased Skp2 stability following wire injury is critical for VSMC proliferation and neointimal hyperplasia formation.

3.9 Skp2 overexpression does not promote VSMC neointimal hyperplasia in FAK-I-treated mice

As Skp2 overexpression showed a slight increase in VSMC proliferation *in vitro* (Figure 5B), we next investigated whether Skp2 overexpression could promote VSMC proliferation in FAK-I-treated mice following wire injury. Myc-Skp2 lentivirus was mixed with Pluronic F-127 and was applied to the outside of femoral arteries immediately following wire injury. However, Skp2 overexpression failed to increase neointimal hyperplasia in FAK-I-treated mice (Supplementary material online, Figure S16A), suggesting that Skp2 overexpression alone is not sufficient for VSMC proliferation *in vivo*. Interestingly, while Myc-Skp2 showed strong expression, as observed by Myc staining, following wire injury (Figure 7 and Supplementary material online, Figure S16B), Myc-Skp2 expression was much lower in sham controls or in FAK-I-treated mice (Figure 7 and Supplementary material online, Figure S16B). Similar to wire injury results in the current study, sham controls and FAK-I-treated mice showed low active pY397 FAK and elevated nuclear FAK (Figure 7 and Supplementary material online, Figure S16C). Skp2 overexpression *in vivo* also did not decrease p27 levels in FAK-I-treated mice following wire injury (Figure 7 and Supplementary material online, Figure S16D). These data demonstrated that concentrated nuclear FAK in VSMCs can still suppress Skp2 levels even under overexpression condition *in vivo* and that Skp2 expression alone is not sufficient to promote VSMC proliferation.

4. Discussion

Cell cycle progression is tightly regulated by the interplay between cell cycle promoting cyclin-CDK complexes and CDKIs. While the role of FAK in proliferation has been more studied in cell cycle promoters, little attention has been paid to FAK regulation of CDKIs. Our study showed that pharmacological and genetic FAK inhibition in VSMCs prevents cell cycle progression through expression of Cip/Kip family CDKIs via regulation of Skp2 stability. It has been suggested that phosphorylation of FAK at pY397 may be important for maintaining Skp2 protein more stable,⁴⁴ but a molecular mechanism of how active FAK regulates Skp2 stability has not been identified. Here we found that inactive nuclear FAK enhances proteasomal degradation of Skp2, which in turn increases expression of the CDKIs p27 and p21. FAK interacts with Skp2 and the APC/C E3 ligase activator Fzr1 via the FAK FERM domain, and FAK nuclear localization was critical for degradation of Skp2 and Fzr1. Overexpression of cyclin D1 alone was not enough to rescue VSMC proliferation in FAK-inhibited condition as cyclin D1 overexpression had no effect on p27 and p21 protein levels. However, overexpression of both Skp2 and cyclin D1 was able to rescue FAK-KD VSMC proliferation *in vitro*. These findings show that the ability of active cytoplasmic FAK to promote proliferation by increasing cell cycle promoting proteins (cyclin D1 and

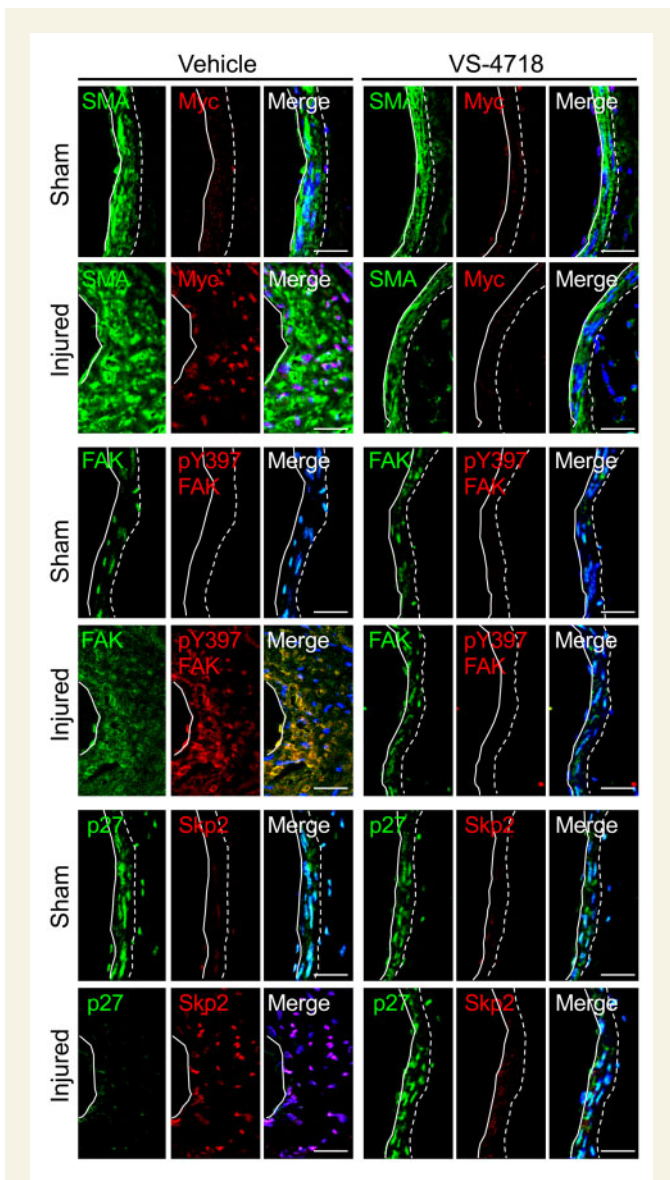


Figure 7 FAK inhibition blocks neointimal hyperplasia in overexpressing Skp2 mice upon wire injury. Femoral arteries were coated with Myc-Skp2 overexpressing lentivirus immediately following wire injury. Mice were treated with vehicle or VS-4718 (50 mg/kg) twice daily. After 2 week wire injury, immunostainings for α -SMA, Myc, FAK, pY397 FAK, p27, and Skp2 were shown. SMA (green), Myc-Skp2 or pY397 FAK (red), and DAPI (blue) were merged ($n = 4$). Dotted line in image marks the external or internal elastic lamina. White line shows endothelial layer. Scale bar: 20 μ m.

Skp2) and reducing cell cycle inhibitors (p27 and p21) makes FAK a key regulator in both regulatory arms of cell cycle progression. Ultimately, forced FAK nuclear localization increases p27 and p21 via loss of Skp2-Fzr1 stability, leading to reduced VSMC proliferation and neointimal hyperplasia upon vessel injury (Supplementary material online, Figure S17).

Skp2 knockdown using shRNA completely blocked injury induced neointimal hyperplasia (Figure 6). Following wire injury, FAK relocated to the cytoplasm and was activated in both shScr and shSkp2 mice, further supporting that FAK cytoplasmic relocalization and subsequent increased Skp2 stability are required for VSMC neointimal hyperplasia

formation. On the other hand, Skp2 overexpression did not overcome forced FAK nuclear localization in FAK-I-treated mice, suggesting that nuclear FAK is a strong suppressor of VSMC proliferation through regulation of cell cycle machineries. While simultaneous overexpression of Skp2 and cyclin D1 could promote proliferation of FAK-KD VSMCs *in vitro* (Figure 5), Skp2 overexpression *in vivo* did not promote VSMC proliferation in control or injured group with FAK-I treatment (Figure 7). This could be simply because FAK still showed some cytoplasmic localization within FAK-KD VSMCs *in vitro* (Supplementary material online, Figure S8). It is possible that growth factors within the serum are enough to promote a subpopulation of FAK-KD to cycle into the cytoplasm which could alleviate some nuclear FAK-mediated suppression of overexpressed Skp2. However, *in vivo*, FAK was almost entirely localized to the nucleus in healthy or FAK-I-treated mice, thus preventing any relief from FAK-mediated Skp2 degradation. Additionally, we previously showed that nuclear FAK regulates VSMC proliferation through degradation of GATA4, thus preventing expression of cyclin D1.³¹ While we overexpressed Skp2 *in vivo*, FAK-I-induced FAK nuclear localization still disrupts the GATA4-cyclin D1 axis, thus blocking VSMC proliferation *in vivo*.

Interestingly, the FAK FERM domain seems to act as a scaffold for the degradation of several nuclear proteins by recruiting substrates and E3 ubiquitin ligases (e.g. p53/mdm2, GATA4/CHIP).^{35,38} The FERM domain indeed serves as a protein degradation platform for Skp2 and Fzr1 (Figure 2). We further characterized FAK's scaffolding role for Skp2 and Fzr1, and found that nuclear export is necessary for their degradation, presumably through the 26S proteasome (Supplementary material online, Figure S17). Additionally, FAK nuclear localization was also critical for potentially priming a degradation complex of Skp2 and Fzr1 in the presence of FAK-I. As FAK is known to shuttle between the cytoplasm and nucleus, it remains to be tested whether FAK physically carries Skp2 and Fzr1 to the cytoplasm or merely primes Skp2-Fzr1 for nuclear export. One question we have not resolved is which E3 ligase is responsible for loss of Fzr1 following FAK inhibition. Several E3 ligases have been targeted for degradation either through modification mediated by an external ligase or they are self-catalysed and be degraded along with their substrates.⁴⁵⁻⁴⁷ As it has been reported that Fzr1 can self-catalyse in G1 phase,^{47,48} it is possible that FAK promotes the self-catalyzation of Fzr1 while simultaneously targeting Skp2 degradation.

The interaction between cyclins, CDKs, and CDKIs is a complex process that is tightly regulated. While we have shown here that nuclear FAK regulates p27 and p21 stability via Skp2, we did not investigate FAK regulation of Skp2-mediated degradation of the CDKI p57, a known Skp2 target.²¹⁻²³ In addition to regulating CDKIs, Skp2 has been shown to bind cyclin A, thus preventing inhibition of cyclin A-CDK complexes by p27.⁴⁹ As the Cip/Kip CDKI family also targets cyclin E-CDK2 complex, FAK catalytic activity may reduce cyclin E expression and CDK2 activity. Further studies are needed to completely elucidate FAK-mediated regulation of both cell cycle promoting and cell cycle inhibitory pathways.

Supplementary material

Supplementary material is available at *Cardiovascular Research* online.

Funding

This work was supported by American Heart Association 12SDG10970000 (to S.L.), 16GRNT30960007 (to S.L.); National Institutes of Health R01

CA190688 (to E.A.), R01 HL136432 (to S.L.); 2019 College of Medicine Intramural grant from University of South Alabama (to S.L.). Nikon A1 Confocal microscope was supported by the National Institutes of Health S10RR027535 (to University of South Alabama).

Conflict of interest: none declared.

Data availability

No new data were generated or analysed in support of this research.

References

- Campbell JH, Campbell GR. Endothelial cell influences on vascular smooth muscle phenotype. *Annu Rev Physiol* 1986;**48**:295–306.
- Bennett MR, Sinha S, Owens GK. Vascular smooth muscle cells in atherosclerosis. *Circ Res* 2016;**118**:692–702.
- Newby AC, Zaltsman AB. Molecular mechanisms in intimal hyperplasia. *J Pathol* 2000;**190**:300–309.
- Gomez D, Owens GK. Smooth muscle cell phenotypic switching in atherosclerosis. *Cardiovasc Res* 2012;**95**:156–164.
- Masiero G, Mojoli M, Ueshima D, Tarantini G. Current concepts on coronary revascularization using BRS in patients with diabetes and small vessels disease. *J Thorac Dis* 2017;**9**:S940–S949.
- Price MJ, Saito S, Shlofmitz RA, Spriggs DJ, Attubato M, McLaurin B, Popma Almonacid A, Brar S, Liu M, Moe E, Mehran R. First report of the resolute Onyx 2.0-mm zotarolimus-eluting stent for the treatment of coronary lesions with very small reference vessel diameter. *JACC Cardiovasc Interv* 2017;**10**:1381–1388.
- Tarantini G, Masiero G, Barioli A, Paradies V, Vlachojannis G, Tellaroli P, di Palma CB, Varricchio G, Ielasi A, Loi A, Steffenino B, Ueshima G, Mojoli D, Smits MP. Absorb bioresorbable vascular scaffold vs. everolimus-eluting metallic stent in small vessel disease: a propensity matched analysis of COMPARE II, RAI, and MAASSTAD-ABSORB studies. *Catheter Cardiovasc Interv* 2018;**92**:E115–E124.
- Brooks RF. Continuous protein synthesis is required to maintain the probability of entry into S phase. *Cell* 1977;**12**:311–317.
- Demasi M, Laurindo FR. Physiological and pathological role of the ubiquitin-proteasome system in the vascular smooth muscle cell. *Cardiovasc Res* 2012;**95**:183–193.
- Gordon D, Reidy MA, Benditt EP, Schwartz SM. Cell proliferation in human coronary arteries. *Proc Natl Acad Sci USA* 1990;**87**:4600–4604.
- Hedin U, Roy J, Tran PK. Control of smooth muscle cell proliferation in vascular disease. *Curr Opin Lipidol* 2004;**15**:559–565.
- Resnitzky D, Gossen M, Bujard H, Reed SI. Acceleration of the G1/S phase transition by expression of cyclins D1 and E with an inducible system. *Mol Cell Biol* 1994;**14**:1669–1679.
- Bertoli C, Skotheim JM, de Bruin RA. Control of cell cycle transcription during G1 and S phases. *Nat Rev Mol Cell Biol* 2013;**14**:518–528.
- Sherr CJ, Roberts JM. CDK inhibitors: positive and negative regulators of G1-phase progression. *Genes Dev* 1999;**13**:1501–1512.
- Musgrove EA, Caldon CE, Barraclough J, Stone A, Sutherland RL. Cyclin D as a therapeutic target in cancer. *Nat Rev Cancer* 2011;**11**:558–572.
- Toyoshima H, Hunter T. p27, a novel inhibitor of G1 cyclin-Cdk protein kinase activity, is related to p21. *Cell* 1994;**78**:67–74.
- Chang MW, Barr E, Lu MM, Barton K, Leiden JM. Adenovirus-mediated over-expression of the cyclin/cyclin-dependent kinase inhibitor, p21 inhibits vascular smooth muscle cell proliferation and neointima formation in the rat carotid artery model of balloon angioplasty. *J Clin Invest* 1995;**96**:2260–2268.
- Chen D, Krasinski K, Sylvester A, Chen J, Nisen PD, Andres V. Downregulation of cyclin-dependent kinase 2 activity and cyclin A promoter activity in vascular smooth muscle cells by p27(KIP1), an inhibitor of neointima formation in the rat carotid artery. *J Clin Invest* 1997;**99**:2334–2341.
- Wakino S, Kintscher U, Kim S, Yin F, Hsueh WA, Law RE. Peroxisome proliferator-activated receptor gamma ligands inhibit retinoblastoma phosphorylation and G1→S transition in vascular smooth muscle cells. *J Biol Chem* 2000;**275**:22435–22441.
- Tanner FC, Boehm M, Akyurek LM, San H, Yang ZY, Tashiro J, Nabel GJ, Nabel EG. Differential effects of the cyclin-dependent kinase inhibitors p27(Kip1), p21(Cip1), and p16(Ink4) on vascular smooth muscle cell proliferation. *Circulation* 2000;**101**:2022–2025.
- Nakayama K, Nagahama H, Minamishima YA, Miyake S, Ishida N, Hatakeyama S, Kitagawa M, Iemura S, Natsume T, Nakayama KI. Skp2-mediated degradation of p27 regulates progression into mitosis. *Dev Cell* 2004;**6**:661–672.
- Bornstein G, Bloom J, Sity-Shevah D, Nakayama K, Pagano M, Hershko A. Role of the SCFskp2 ubiquitin ligase in the degradation of p21Cip1 in S phase. *J Biol Chem* 2003;**278**:25752–25757.
- Kamura T, Hara T, Kotoshiba S, Yada M, Ishida N, Imaki H, Hatakeyama S, Nakayama K, Nakayama KI. Degradation of p57Kip2 mediated by SCFskp2-dependent ubiquitylation. *Proc Natl Acad Sci USA* 2003;**100**:10231–10236.
- Mitra SK, Hanson DA, Schlaepfer DD. Focal adhesion kinase: in command and control of cell motility. *Nat Rev Mol Cell Biol* 2005;**6**:56–68.
- Mitra SK, Schlaepfer DD. Integrin-regulated FAK-Src signaling in normal and cancer cells. *Curr Opin Cell Biol* 2006;**18**:516–523.
- Calalb MB, Polte TR, Hanks SK. Tyrosine phosphorylation of focal adhesion kinase at sites in the catalytic domain regulates kinase activity: a role for Src family kinases. *Mol Cell Biol* 1995;**15**:954–963.
- Morla AO, Mogford JE. Control of smooth muscle cell proliferation and phenotype by integrin signaling through focal adhesion kinase. *Biochem Biophys Res Commun* 2000;**272**:298–302.
- Taylor JM, Mack CP, Nolan K, Regan CP, Owens GK, Parsons JT. Selective expression of an endogenous inhibitor of FAK regulates proliferation and migration of vascular smooth muscle cells. *Mol Cell Biol* 2001;**21**:1565–1572.
- Bae YH, Mui KL, Hsu BY, Liu SL, Cretu A, Razinia Z, Xu T, Pure E, Assoian RK. A FAK-Cas-Rac-lamellipodin signaling module transduces extracellular matrix stiffness into mechanosensitive cell cycling. *Sci Signal* 2014;**7**:ra57.
- Mui KL, Bae YH, Gao L, Liu SL, Xu T, Radice GL, Chen CS, Assoian RK. N-cadherin induction by ECM stiffness and FAK overrides the spreading requirement for proliferation of vascular smooth muscle cells. *Cell Rep* 2015;**10**:1477–1486.
- Jeong K, Kim JH, Murphy JM, Park H, Kim SJ, Rodriguez YAR, Kong H, Choi C, Guan JL, Taylor JM, Lincoln TM, Gerthoffer WT, Kim JS, Ahn EE, Schlaepfer DD, Lim SS. Nuclear focal adhesion kinase controls vascular smooth muscle cell proliferation and neointimal hyperplasia through GATA4-mediated cyclin D1 transcription. *Circ Res* 2019;**125**:152–166.
- Koyama H, Raines EW, Bornfeldt KE, Roberts JM, Ross R. Fibrillar collagen inhibits arterial smooth muscle proliferation through regulation of Cdk2 inhibitors. *Cell* 1996;**87**:1069–1078.
- Braun-Dullaeus RC, Mann MJ, Ziegler A, von D. L H, Dzau VJ. A novel role for the cyclin-dependent kinase inhibitor p27(Kip1) in angiotensin II-stimulated vascular smooth muscle cell hypertrophy. *J Clin Invest* 1999;**104**:815–823.
- Ilic D, Almeida EA, Schlaepfer DD, Dazin P, Aizawa S, Damsky CH. Extracellular matrix survival signals transduced by focal adhesion kinase suppress p53-mediated apoptosis. *J Cell Biol* 1998;**143**:547–560.
- Lim ST, Chen XL, Lim Y, Hanson DA, Vo TT, Howerton K, Larocque N, Fisher SJ, Schlaepfer DD, Ilic D. Nuclear FAK promotes cell proliferation and survival through FERM-enhanced p53 degradation. *Mol Cell* 2008;**29**:9–22.
- Allagnat F, Dubuis C, Lambelet M, Le GL, Alonso F, Corpataux JM, Deglise S, Haefliger JA. Connexin37 reduces smooth muscle cell proliferation and intimal hyperplasia in a mouse model of carotid artery ligation. *Cardiovasc Res* 2017;**113**:805–816.
- Braun-Dullaeus RC, Mann MJ, Dzau VJ. Cell cycle progression: new therapeutic target for vascular proliferative disease. *Circulation* 1998;**98**:82–89.
- Lim ST, Miller NL, Chen XL, Tancioni I, Walsh CT, Lawson C, Uryu S, Weis SM, Cheresch DA, Schlaepfer DD. Nuclear-localized focal adhesion kinase regulates inflammatory VCAM-1 expression. *J Cell Biol* 2012;**197**:907–919.
- Thiagarajan PS, Sinyuk M, Turaga SM, Mulkearns-Hubert EE, Hale JS, Rao V, Demelash A, Saygin C, China A, Alban TJ, Hitomi M, Torre-Healy LA, Alvarado AG, Jarrar A, Wiechert A, Adorno-Cruz V, Fox PL, Calhoun BC, Guan JL, Liu H, Reizes O, Lathia JD. Cx26 drives self-renewal in triple-negative breast cancer via interaction with NANOG and focal adhesion kinase. *Nat Commun* 2018;**9**:578.
- Canel M, Byron A, Sims AH, Cartier J, Patel H, Frame MC, Brunton VG, Serrels B, Serrels A. Nuclear FAK and Runx1 cooperate to regulate IGFBP3, cell-cycle progression, and tumor growth. *Cancer Res* 2017;**77**:5301–5312.
- Bashir T, Dorrello NV, Amador V, Guardavaccaro D, Pagano M. Control of the SCF(Skp2-Cks1) ubiquitin ligase by the APC/C(Cdh1) ubiquitin ligase. *Nature* 2004;**428**:190–193.
- Wu YJ, Bond M, Sala-Newby GB, Newby AC. Altered S-phase kinase-associated protein-2 levels are a major mediator of cyclic nucleotide-induced inhibition of vascular smooth muscle cell proliferation. *Circ Res* 2006;**98**:1141–1150.
- Kee N, Sivalingham S, Boonstra R, Wojtowicz JM. The utility of Ki-67 and BrdU as proliferative markers of adult neurogenesis. *J Neurosci Methods* 2002;**115**:97–105.
- Bond M, Sala-Newby GB, Newby AC. Focal adhesion kinase (FAK)-dependent regulation of S-phase kinase-associated protein-2 (Skp-2) stability. A novel mechanism regulating smooth muscle cell proliferation. *J Biol Chem* 2004;**279**:37304–37310.
- Ryan PE, Davies GC, Nau MM, Lipkowitz S. Regulating the regulator: negative regulation of Cbl ubiquitin ligases. *Trends Biochem Sci* 2006;**31**:79–88.
- Fang S, Jensen JP, Ludwig RL, Vousden KH, Weissman AM. Mdm2 is a RING finger-dependent ubiquitin protein ligase for itself and p53. *J Biol Chem* 2000;**275**:8945–8951.
- de Bie P, Ciechanover A. Ubiquitination of E3 ligases: self-regulation of the ubiquitin system via proteolytic and non-proteolytic mechanisms. *Cell Death Differ* 2011;**18**:1393–1402.
- Listovsky T, Oren YS, Yudkovsky Y, Mahbubani HM, Weiss AM, Lebediker M, Brandeis M. Mammalian Cdh1/Fzr mediates its own degradation. *EMBO J* 2004;**23**:1619–1626.
- Ji P, Goldin L, Ren H, Sun D, Guardavaccaro D, Pagano M, Zhu L. Skp2 contains a novel cyclin A binding domain that directly protects cyclin A from inhibition by p27Kip1. *J Biol Chem* 2006;**281**:24058–24069.

Translational perspective

Increased VSMC proliferation contributes to pathological vessel narrowing in atherosclerosis and following vascular interventions. Blocking VSMC proliferation will reduce atherosclerosis progression and increase patency of vascular interventions. We found that forced nuclear FAK localization by FAK inhibition reduced VSMC proliferation upon vessel injury. Nuclear FAK decreased Skp2 protein expression by proteasomal degradation, thereby increasing the expression of cell cycle inhibitors p27 and p21 and blocking cell cycle progression. This study has demonstrated the potential for FAK inhibitors in blocking VSMC proliferation to treat vessel narrowing diseases.